

See discussions, stats, and author profiles for this publication at: <https://www.researchgate.net/publication/257124797>

# Comparative study on the transition metal complexes of a novel thiacalix[4]arene derivative

ARTICLE *in* CHEMICAL PHYSICS · JANUARY 2006

Impact Factor: 1.65 · DOI: 10.1016/j.chemphys.2005.07.024

CITATIONS

6

READS

9

6 AUTHORS, INCLUDING:



**Akapong Suwattanamala**

Burapha University

7 PUBLICATIONS 67 CITATIONS

SEE PROFILE



**Marco Wenzel**

Technische Universität Dresden

46 PUBLICATIONS 984 CITATIONS

SEE PROFILE



**Alexandre L Magalhães**

REQUIMTE, University of Porto, Portugal

67 PUBLICATIONS 799 CITATIONS

SEE PROFILE



**José Ferreira Gomes**

University of Porto

72 PUBLICATIONS 1,003 CITATIONS

SEE PROFILE

## Comparative study on the transition metal complexes of a novel thiacalix[4]arene derivative

A. Suwattanamala<sup>a</sup>, D. Appelhans<sup>b</sup>, M. Wenzel<sup>c</sup>, K. Gloe<sup>c</sup>,  
A.L. Magalhães<sup>a,\*</sup>, J.A.N.F. Gomes<sup>a</sup>

<sup>a</sup> REQUIMTE, Departamento de Química, Faculdade de Ciências, Universidade do Porto, Rua do Campo Alegre, 687, 4169-007 Porto, Portugal

<sup>b</sup> Leibniz Institute of Polymer Research Dresden, Hohe Strasse 6, 01069 Dresden, Germany

<sup>c</sup> Institute of Inorganic Chemistry, TU Dresden, 01062 Dresden, Germany

Received 11 April 2005; accepted 6 July 2005

Available online 15 August 2005

### Abstract

A comparative study on  $\text{Zn}^{2+}$  and  $\text{Cu}^{2+}$  complexes of the novel compound 5,11,17,23-tetra-*tert*-butyl-25,27-bis{[4-(methoxycarbonyl)phenyl]methoxy}-2,8,14,20-tetrathiacalix[4]arene, that possesses potential as a core unit for the construction of molecular receptors, is presented using semiempirical AM1 calculation. The possible structures of each metal complex and their corresponding energetic data are compared with the parent 5,11,17,23-tetra-*tert*-butyl-2,8,14,20-tetrathiacalix[4]arene. The complexation ability of both thiacalix[4]arenes towards the two metal ions is discussed on the basis of binding energies. Both thiacalix[4]arene 1:1 complexes show higher complexation ability towards  $\text{Cu}^{2+}$ . However, 5,11,17,23-tetra-*tert*-butyl-25,27-bis{[4-(methoxycarbonyl)phenyl]methoxy}-2,8,14,20-tetrathiacalix[4]arene presents lower complexation ability when compared with the 5,11,17,23-tetra-*tert*-butyl-2,8,14,20-tetrathiacalix[4]arene. The results of liquid–liquid extraction experiments of the thiacalix[4]arenes are in good agreement with the theoretical calculations.

© 2005 Elsevier B.V. All rights reserved.

**Keywords:** Thiacalix[4]arenes; Metal complex; Complexation ability; AM1 calculations; Liquid–liquid extraction

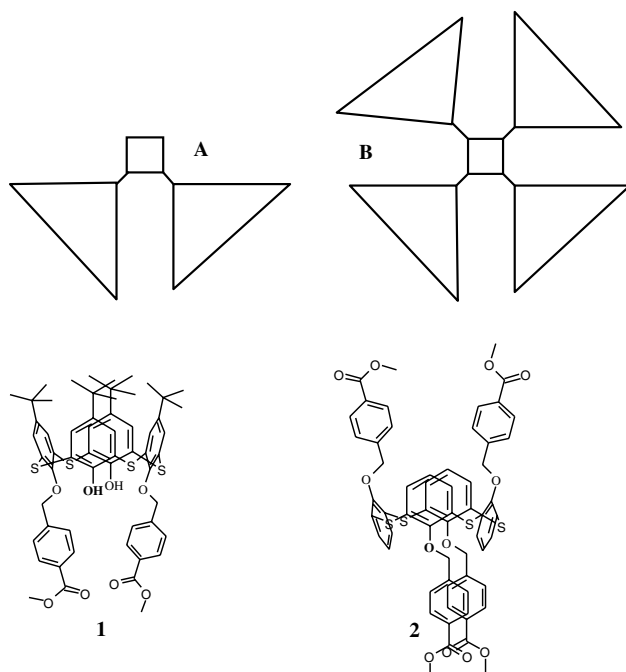
### 1. Introduction

The construction and control of three-dimensional molecular structures with complexing properties are research topics in dendrimer and supramolecular chemistry mimicking the function of biomolecules [1,2]. Due to the macrocyclic structure and simple modification of the phenol unit, calixarenes have been used as a scaffold to construct artificial enzymes for chemical transformation and molecular recognition [3]. In the last decade, thiacalixarenes were reported as new compounds in the family of calixarenes substituting only

the bridging methylene groups between the phenolic units by sulfur atoms [4]. In particular, thiacalix[4]arenes have been proposed as precursors for potential applications based on (a) the large diversity in host–guest properties [5] due to the increasing number of coordination sites in the lower and upper rims and, (b) the versatile use in the construction of different and stable conformers [6]. Therefore, the thiacalix[4]arene is suited to support the formation of different molecular shapes with complexing thiacalixarene moieties as central unit for the construction of dendritic-shelled molecular receptors, shown in Scheme 1, to enhance the stability of host–guest interactions, e.g., towards biological environment. Theoretical calculations are used nowadays to describe the metal complexation of core units 1 and 2 [6c] in Scheme 1, to optimize

\* Corresponding author. Tel.: +351 226 082804; fax: +351 226 082959.

E-mail address: [almagalh@fc.up.pt](mailto:almagalh@fc.up.pt) (A.L. Magalhães).



Scheme 1. Thiocalix[4]arene derivatives **1** and **2** suited for the construction of dendritic shelled molecular receptors **A**, consisting of core unit and two dendritic wedges, and **B**, consisting of core unit and four dendritic wedges.

and minimize the synthetic work with such large molecules.

Recently, density functional theory (DFT) methodology has been successfully applied in the theoretical study of structure and conformational equilibrium of thiocalix[4]arene [7] and of tetraamino- and tetramercaptothiocalix[4]arenes [8]. Complexation features of parent 5,11,17,23-tetra-*tert*-butyl-2,8,14,20-tetrathiacalix[4]arene **3** and other thiocalix[4]arene derivatives towards transition metals and lanthanide ions were intensively explored indicating potential applications [9–12]. On the other hand, zinc has been recognized as an important metal in catalysis, metalloenzymes, macrocyclic ligands and bioinorganic systems [13,14]. Therefore, a strong motivation emerged to investigate structural and energetic data of **3** and its Zn complexes using high-level DFT calculations [15]. In particular, the calculations revealed that the Zn complexation with **3** is realized by a twofold deprotonated ligand shown in Fig. 1. This result supports the coordination of complexed  $\text{Zn}^{2+}$  with **3** in solid state [16], and will be assumed also for complexes of transition metals with **3** under basic condition in solution [10]. In addition, the complexes of the novel thiocalix[4]arene derivatives as tetraaminothiocalix[4]arene, tetraamino-*p*-*tert*-butylthiocalix[4]arene with  $\text{Zn}^{2+}$  were recently studied by quantum chemical calculations [17,18]. The application of high-level DFT calculations would be clearly desirable in order to work with more realistic molecular models, but is prohibitive because

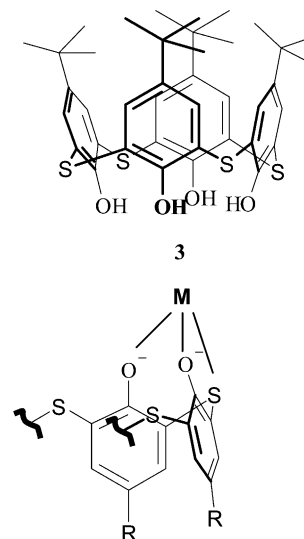


Fig. 1. Coordinated Zn(II) with 5,11,17,23-tetra-*tert*-butyl-2,8,14,20-tetrathiacalix[4]arene (compound **3**). For clarity, partly drawing of **3**. General assumption of coordinated metals with thiocalix[4]arene in [10].

of the huge computer time required for the geometry optimizations. Considering the big size of the molecular systems in this work, semiempirical methods seem to be the alternative choice. The AM1 Hamiltonian [19–21] has already been employed in the structural and energetic studies of zinc complexes with supramolecular structures as for example porphyrin [22–24]. In particular, it has been applied successfully in the study of zinc complexes with sulfur containing calix[4]arenes, whose results showed a good agreement with X-ray data [25]. In addition, a new reparameterization of AM1 applied to transition metals [26] has been implemented in the recent version of the Molecular Orbital Package 2002 (MOPAC 2002) [27], and it is employed in the current study.

In this work, the structures and energetics of 5,11,17,23-tetra-*tert*-butyl-25,27-bis{[4-(methoxycarbonyl)phenyl]methoxy}-2,8,14,20-tetrathiacalix[4]arene **1** were investigated. The comparative study on its complexation ability towards the transition metals ions  $\text{Zn}^{2+}$  and  $\text{Cu}^{2+}$  were performed and also compared with **3** at the same level. The main goal of this work is to enhance the understanding of the characteristic host–guest interactions of the substructure **1** in novel molecular receptors, shown in Scheme 1, towards transition metals. The theoretical calculations aim to find suitable and effectual metal coordinations of **1** in the gas phase. Further, the results of metal complexes with **3** are compared with the previous theoretical calculations obtained by DFT. Liquid–liquid extraction experiments of **1** and **3** towards transition metal ions were also carried out and the results were used to support the semiempirical calculations. This study will be helpful for us to clarify the

extraction properties of novel lysine dendrimers [28] with the substructure **1** as core unit towards  $\text{Zn}^{2+}$  and  $\text{Cu}^{2+}$  in a forthcoming study.

## 2. Computational method

The molecular geometries for *cone* conformer of **1** and **3** were obtained by complete optimization at the semiempirical level using the AM1 method [19–21]. The first and second deprotonated forms were optimized at the same level, and the structures of each species were analyzed in detail. The  $\text{Zn}^{2+}$  and  $\text{Cu}^{2+}$  ions were selected to carry out a comparative study on the complexation ability of the twofold deprotonated species of each compound towards transition metals. This type of molecular systems possess many local minima but our interest is restricted to the characterization of the most stable complexes with the coordination at the lower rim. Therefore, different structures were considered as starting points for the complete geometry optimization procedures based on distinct type of cation binding sites. The geometry optimizations were carried out with the Baker's eigenvector following algorithm [29] at the AM1 method which was parameterized for both metal ions in the recent version of MOPAC 2002 program [27]. In order to improve the quality of the results, additional single point calculations at the B3LYP/6-31G(d) level [30,31] with the AM1 optimized structures (B3LYP/6-31G(d)//AM1) were also performed using the GAUSSIAN 2003 program package [32]. The RB3LYP/DFT calculations using singlet spin multiplicity were carried out for the  $\text{Zn}^{2+}$  complexes whereas the UB3LYP/DFT calculations using doublet spin multiplicity were performed for the  $\text{Cu}^{2+}$  complexes. The binding energy of each complex was calculated as the difference between the total energy of the optimized structure in vacuum and the sum of the energies of the most stable structures of the isolated moieties.

## 3. Experimental method

The liquid–liquid extraction experiments were performed at  $22 \pm 1^\circ\text{C}$  in microcentrifuge tubes ( $2\text{ cm}^3$ ) by means of mechanical overhead shaking. The phase ratio  $V_{(\text{w})}:V_{(\text{org})}$  (500  $\mu\text{l}$  each) was 1:1. The shaking time was chosen as 30 min for the Cu and Zn experiments, because the equilibrium was reached in this period. A shaking time of 24 h was chosen for the extraction measurements from the metal ion mixture of  $\text{Co}^{2+}$ ,  $\text{Ni}^{2+}$ ,  $\text{Cu}^{2+}$ ,  $\text{Zn}^{2+}$  and  $\text{Cd}^{2+}$ . After the extraction, all samples were centrifuged and the phases separated. In case of Zn experiments, the metal concentration was detected in both phases radiometrically by  $\gamma$ -radiation of  $^{65}\text{Zn}$  in a NaI (TI) scintillation counter (Cobra II/Canberra-

Packard). The Cu concentration as well as all metal ion concentrations in the multi-element experiments were determined by ICP-MS (ICP-MS-ELAN 9000/Perkin–Elmer) measurements of the aqueous phase. The pH of aqueous solution was adjusted using 4-morpholinoethanesulfonic acid (MES)/NaOH and 4-(2-hydroxyethyl)-1-piperazineethanesulfonic acid (HEPES)/NaOH buffer solutions.

## 4. Results and discussion

### 4.1. Structure and hydrogen bonding of **1** and **3**

The first deprotonation of **1** and **3** resulted in only one molecular structure for each compound. However, concerning the second deprotonation, one and two possible structures were obtained with **1** and **3**, respectively. In **3** both deprotonated phenol groups can either be adjacent (first pattern, **I**) or opposite (second pattern, **II**), whereas for **1** only the pattern **II** was found (see Figs. 2 and 3).

The AM1 optimized structure of *cone* conformer of **3** in neutral ( $\text{LH}_4$ ), first ( $\text{LH}_3^-$ ) and second ( $\text{LH}_2^{2-}$ ) deprotonation forms are presented in Fig. 2. The corresponding total energies obtained with B3LYP/6-31G(d)//AM1 method are  $-3446.803917$ ,  $-3446.262402$ ,  $-3445.610627$  and  $-3445.615148$  hartree, respectively. Some relevant geometric parameters of all the species are available as [Supplementary material](#). Although the structures predicted in gas phase can not be directly compared with those obtained experimentally in condensed phase there is a good agreement between theoretical calculations and X-ray crystallography data for most of the bond distances in  $\text{LH}_4$  species. The AM1 calculations overestimate all the bond angles by ca.  $4.0^\circ$ , except the C–C–O angles which are predicted to be smaller by the same amount. The neutral form possesses  $\text{C}_4$  symmetry, as it was observed in previous X-ray crystals [33]. This is confirmed by the same value obtained for both the  $\text{O}_1\text{--O}_3$  and  $\text{O}_2\text{--O}_4$  distances, and the similarity of the two angles  $\phi$  between opposite phenol units, though the AM1 predictions overestimate the values of the latter parameter by about  $10.0^\circ$ . The structural parameters for the  $\text{LH}_4$  species are also in a good agreement with a previous study done at B3LYP/6-31G(d) level [15]. These results validate the AM1 method and show that it can be applied for the study of molecular systems based on thiacalix[4]arene. The majority of the geometric parameters are not influenced by the deprotonation process except the C–O and O–O bond distances and the C–C–O bond angles. The C–O distance of the phenolate is reduced by about  $0.10\text{ \AA}$ , whereas the C–C–O angle is increased by ca.  $5.0^\circ$  in both  $\text{LH}_3^-$  and  $\text{LH}_2^{2-}$  species when compared with  $\text{LH}_4$ .

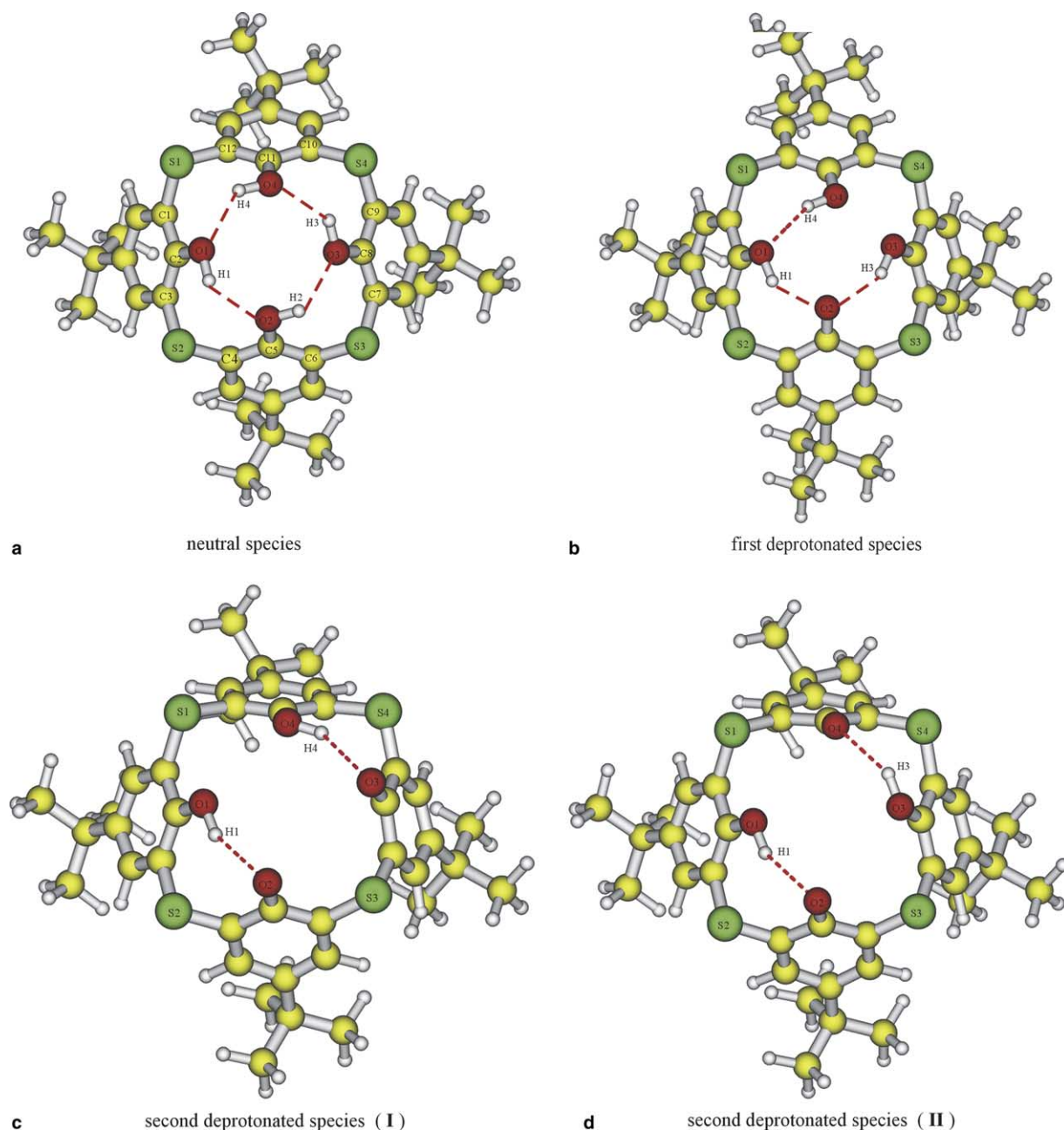


Fig. 2. AM1 optimized structures of neutral and deprotonated species for *cone* conformer of 5,11,17,23-tetra-*tert*-butyl-2,8,14,20-tetrathiacalix[4]arene (compound 3).

The optimized structures of the neutral ( $\text{LH}_2$ ), first ( $\text{LH}^-$ ) and second ( $\text{L}^{2-}$ ) deprotonation forms of **1** are shown in Fig. 3, and the corresponding total energies obtained by the same method are  $-4443.210894$ ,  $-4442.665062$  and  $-4442.046783$  hartree, respectively. The values of some relevant structural parameters are available as [Supplementary material](#). The *cone* conformer of the neutral form possesses a  $\text{C}_2$ -like symmetry. The majority of the bond distances are unchanged upon deprotonation, except the C–O and O–O distances. The C–O bond of phenolate is reduced by about  $0.10 \text{ \AA}$  in

both  $\text{LH}^-$  and  $\text{L}^{2-}$  species, when compared with the neutral species. The C–C–O angle of the phenolate is increased by ca.  $5.0^\circ$  in both deprotonated structures. The C–C–O<sub>1</sub> angle of the ether oxygen seems to remain unchanged under the deprotonation process, which contrasts with the change in the C–C–O<sub>3</sub> angle. The size of the *cone* cavity which is related to the distances between the two distal opposite sulfur atoms (S<sub>1</sub>–S<sub>3</sub> and S<sub>2</sub>–S<sub>4</sub>), is an interesting property of thiacalix[4]arene molecules. The S<sub>1</sub>–S<sub>3</sub> distance was reduced while the S<sub>2</sub>–S<sub>4</sub> distance was increased upon first and second



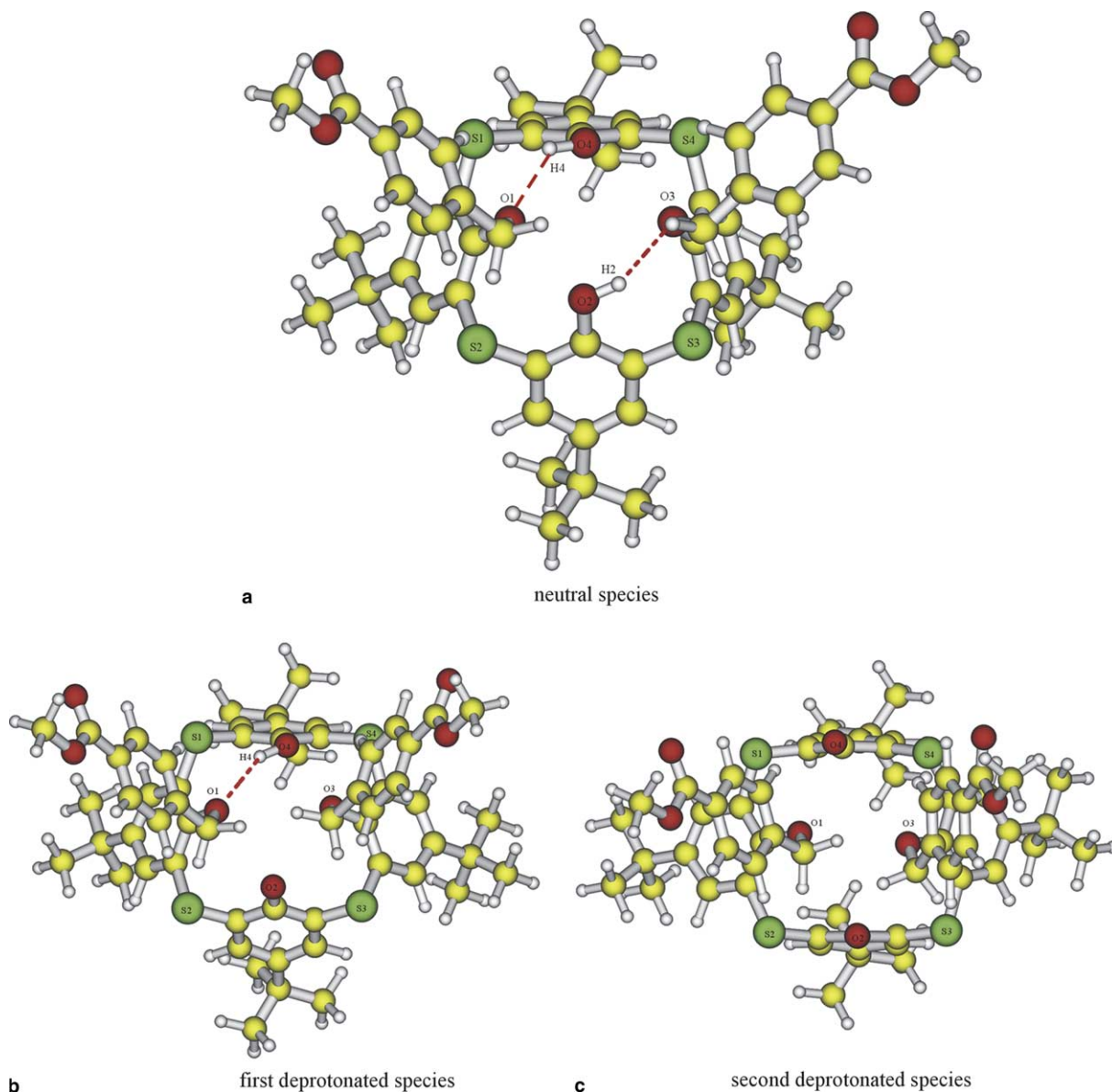


Fig. 3. AM1 optimized structures of neutral and deprotonated species of 5,11,17,23-tetra-*tert*-butyl-25,27-bis{[4-(methoxycarbonyl)phenyl]methoxy}-2,8,14,20-tetrathiocalix[4]arene (compound **1**).

deprotonation of both compounds; the only exception is the  $L^{2-}$  species of **1**. Interestingly, the cavity size of the neutral species of both compounds seems to be identical, despite the modification at the lower rim in **1**.

As expected, the optimized structures present an array of hydrogen bonds that contribute dominantly to stabilize the species of **1** and **3** (see Figs. 2 and 3). Two different possible structures for the second deprotonation were observed in **3**, which have never been referred to in previous studies [10,15]. Structure with pattern **I** shows two adjacent deprotonated phenol groups (see Fig. 2(c)) and it is less stable by ca. 3.0 kcal/mol than **II**, which presents two opposite deprotonated phenol groups (see Fig. 2(d)). This can be rationalized by the weaker repulsion felt by the negative

phenolate groups in opposite than in adjacent positions. Obviously, due to the benzyl-substituent at the lower rim of **1**, only the structure with opposite deprotonated phenol groups was obtained. The number of hydrogen bonds between hydroxyl groups is reduced from four to three and two, respectively, when first and second deprotonations occur in the neutral form of **3**. On the other hand, upon deprotonation of **1** the number of hydrogen bonds are reduced from two in the  $LH_2$  form to one and none in  $LH^-$  and  $L^{2-}$  species, respectively. The hydrogen bonding parameters for each species are gathered in Table 1. The hydrogen bond distances seem to be shorter in the deprotonated species, while the hydrogen bond angles increase when compared with the neutral form of **3**. No relevant difference was found

Table 1

AM1 optimized hydrogen bonding parameters for all the neutral and deprotonation forms of *cone* conformer of **1** and **3**

	Compound <b>1</b> (AM1)			Compound <b>3</b> (AM1)				B3LYP/6-31G(d) <sup>a</sup>
	LH <sub>2</sub>	LH <sup>−</sup>	L <sup>2−</sup>	LH <sub>4</sub>	LH <sub>3</sub> <sup>−</sup>	LH <sub>2</sub> <sup>2−</sup> (1st)	LH <sub>2</sub> <sup>2−</sup> (2nd)	LH <sub>4</sub>
<i>Bond distance (Å)</i>								
O <sub>1</sub> –H <sub>1</sub>				0.98	0.99	0.99	0.99	0.99
H <sub>1</sub> –O <sub>2</sub>				2.12	1.97	2.00	2.04	1.82
O <sub>2</sub> –H <sub>2</sub>	0.98			0.98				0.99
H <sub>2</sub> –O <sub>3</sub>	2.19			2.12				1.82
O <sub>3</sub> –H <sub>3</sub>				0.98	0.99		0.99	0.99
H <sub>3</sub> –O <sub>4</sub>				2.12			2.04	1.82
H <sub>3</sub> –O <sub>2</sub>					2.02			
O <sub>4</sub> –H <sub>4</sub>	0.98	0.98		0.98	0.98	0.99		0.99
H <sub>4</sub> –O <sub>1</sub>	2.14	2.22		2.12	2.10			1.82
H <sub>4</sub> –O <sub>3</sub>						2.00		
<i>Bond angle (°)</i>								
O <sub>1</sub> –H <sub>1</sub> –O <sub>2</sub>				130.6	128.6	154.0	153.4	153.2
O <sub>2</sub> –H <sub>2</sub> –O <sub>3</sub>	148.5			130.2				153.2
O <sub>3</sub> –H <sub>3</sub> –O <sub>4</sub>				130.5			152.7	153.2
O <sub>3</sub> –H <sub>3</sub> –O <sub>2</sub>					139.9			
O <sub>4</sub> –H <sub>4</sub> –O <sub>1</sub>	128.0	149.4		130.1	154.1			153.2
O <sub>4</sub> –H <sub>4</sub> –O <sub>3</sub>						153.2		

<sup>a</sup> Ref. [15].

between the two forms of the second deprotonation. On the contrary, for **1**, all these parameters increase their values during the deprotonation process.

#### 4.2. Structure analysis of the metal complexes

From previous extraction experiments [9], it is suggested that a 1:1 complex  $[M^{2+}H_2L^{2-}]$  of **3** is formed, where  $M^{2+}$  and  $H_2L^{2-}$  denote the metal ion and the twofold deprotonated form of the ligand, respectively. Two possibilities of the twofold deprotonated structures, with either adjacent or opposite phenol groups, were found in the previous section, therefore the structural analysis of the complexes will concern both patterns. The optimized structures of the complexes between the first pattern, (adjacent phenolate groups) and the  $Zn^{2+}$  and  $Cu^{2+}$  ions are shown in Fig. 4. The two adjacent phenolate groups and one bridging sulfur atom show a dominant role in the coordination of the  $Zn^{2+}$  metal ion, enabling the formation of a set of two five membered rings. This complex exhibits two different arrays of hydrogen bonds labelled 1st possibility and 2nd possibility (see Figs. 4(a) and (b)), which are almost identical in energy (the former is only 0.02 kcal/mol more stable). Only the 2nd possibility was obtained in a previous study at B3LYP/6-31G(d) level [15]. The two corresponding structures in the case of the  $Cu^{2+}$  complexes are shown in Figs. 4(c) and (d). The former is also more stable by ca. 1.0 kcal/mol than the latter. This is not surprising because we are dealing with a very flexible molecular system which possesses a lot of local minima in the energy profile. It is suggested that the

migration of protons can easily occur and results in the interconversion of both structures. Other reasonable possibilities for the metal ion coordination were considered for geometry optimization but no additional stable structures were found for both  $Zn^{2+}$  and  $Cu^{2+}$  complexes.

The second deprotonation on opposite phenol groups was also investigated in detail for the metal complexes, which constitutes a 3rd possibility for the 1:1 complex never mentioned previously, and the corresponding optimized structures are presented in Figs. 5(a) and (b). The complexes of both metals show different structural features when compared with the previous ones. The  $Zn^{2+}$  seems to adopt a distorted square planar coordination with the two opposite phenolate groups and two sulfur atoms (see Fig. 5(a)), whereas  $Cu^{2+}$  is coordinated by four oxygen atoms, two phenol and two phenolate groups, in a distorted square planar configuration (see Fig. 5(b)). The geometric parameters of these complexes are gathered in Table 2. Another possible metal coordination involving one sulfur atom, one phenol and one phenolate group was also considered in the structural analysis. However, only in the case of the  $Cu^{2+}$  ion a stable structure was achieved but much higher in energy than those obtained previously.

In addition, a X-ray crystal experiment has revealed a double-cone structure for various metal complexes of **3** [16,34,35], which alternatively suggests that the extracted species may occur as 2:2 complexes  $[M_2(H_2L)_2]$  having a similar double-cone structure. AM1 calculations were also performed for this possibility and the optimized structures of both  $Zn^{2+}$  and  $Cu^{2+}$  complexes

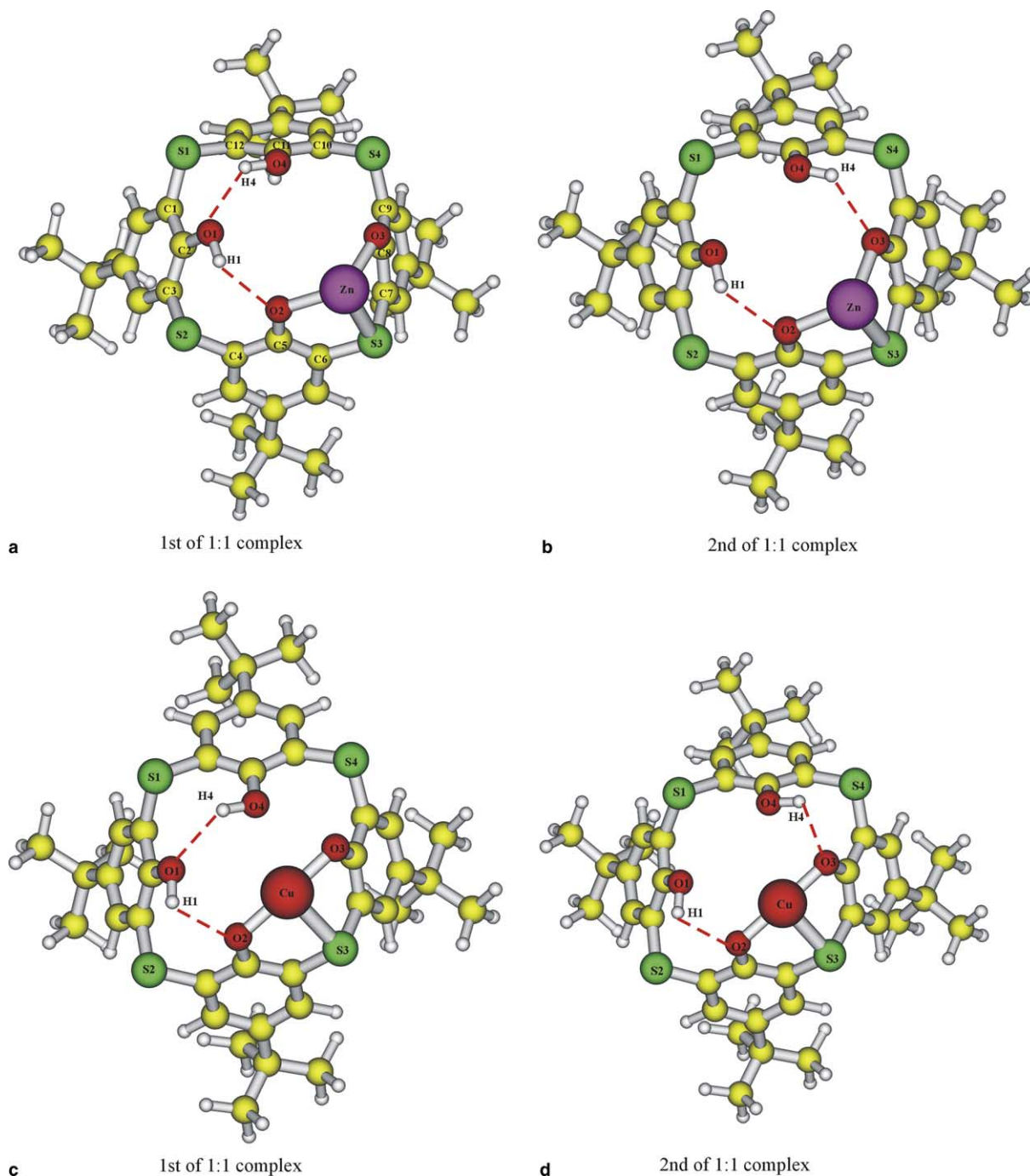


Fig. 4. Optimized structures of 1st and 2nd possibilities of 1:1  $\text{Zn}^{2+}$  and  $\text{Cu}^{2+}$  complexes of **3** obtained at AM1 method.

are presented in Figs. 6(a) and (b), respectively. The optimized structures are in good correspondence to the previous proposals [10], i.e., two dianions  $\text{H}_2\text{L}^{2-}$  connecting to each other via coordination of two metal ions ( $\text{Zn}^{2+}$  or  $\text{Cu}^{2+}$ ) using  $\text{O}^-$ , S,  $\text{O}^-$  donor sets. The remaining protons on the two phenol oxygens may be stabilized by hydrogen bonding to the neighboring phenolate oxygens. Structural parameters of each 2:2 complex are

shown in Table 2 and the number of each atom is referred to Fig. 6(c).

Concerning the novel compound **1** [6c], it can be assumed from our experimental study that the extracted species is a 1:1 complex  $[\text{M}^{2+}\text{L}^{2-}]$ , where  $\text{M}^{2+}$  and  $\text{L}^{2-}$  denote the metal ion and the twofold deprotonated species of **1**, respectively. The optimized structures of each metal complex are shown in Figs. 5(c) and (d). It is interesting to



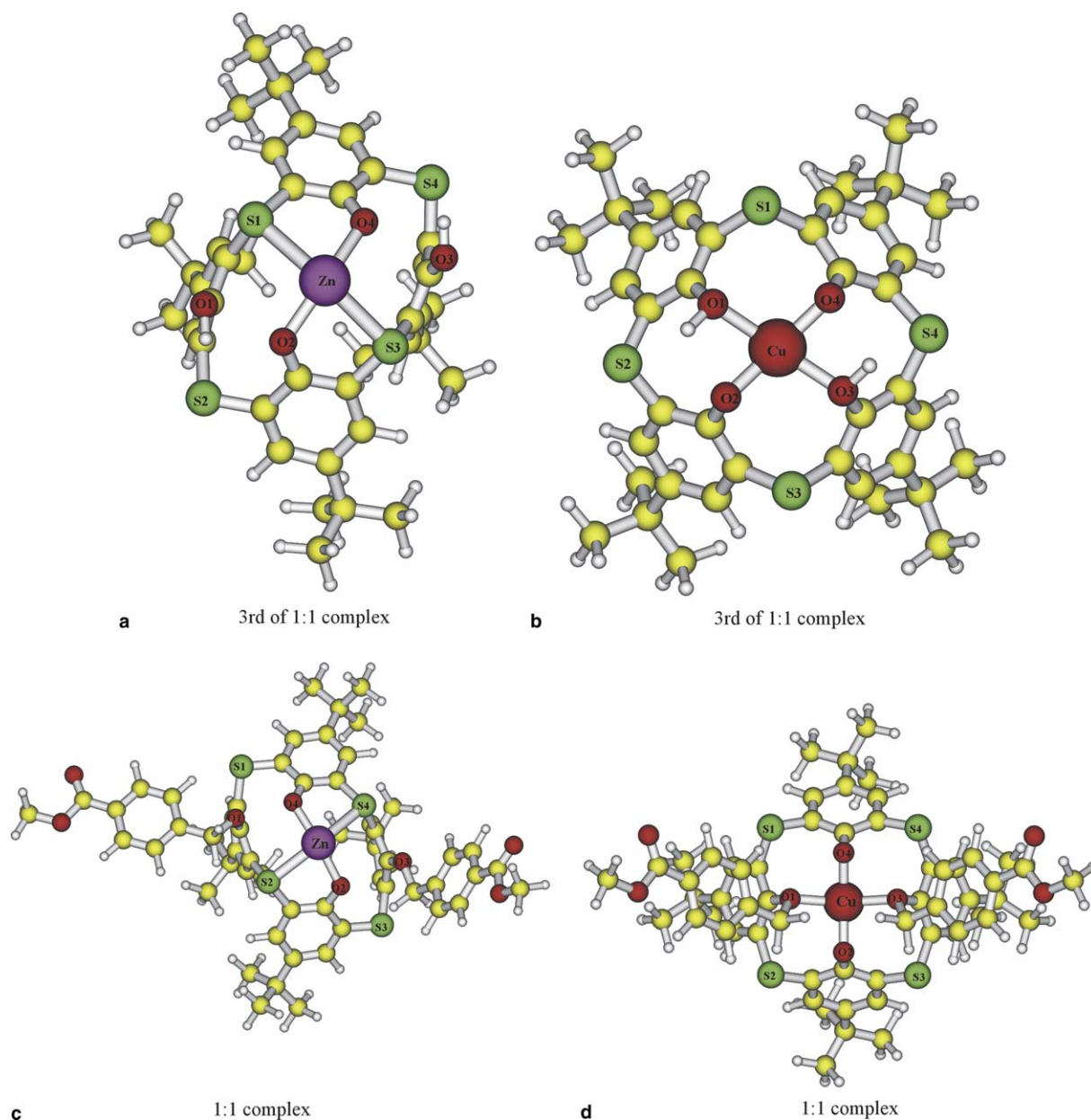


Fig. 5. Optimized structures of 3rd possibility of 1:1 complexes of **3**, (a) and (b); optimized structures of each metal complex of **1** obtained at AM1 method, (c) and (d).

note that the structures of both  $\text{Zn}^{2+}$  and  $\text{Cu}^{2+}$  complexes are similar to the complexation between the metal ions and the second deprotonation on opposite phenol groups of **3** (Figs. 5(a) and (b)). This may suggest that the complex structure pattern depends on the position of the deprotonated phenols. The steric hindrance of bulky groups at lower rim does not modify the structural pattern of the complex. Although other alternative coordination schemes concerning the contribution of bridging sulfur, ether oxygen and phenolate oxygen were also investigated, they were energetically less favourable than those presented before. Therefore, they will not be considered in this comparative study.

Some relevant geometric parameters of the complexes are gathered in Table 2. The AM1 seems to overestimate the values of almost all the parameters except the M–O distances when compared with X-ray crystallography results of the 1:1  $\text{Zn}^{2+}$  complex. Almost all the parameter values in the  $\text{Cu}^{2+}$  complex are smaller than in the  $\text{Zn}^{2+}$  complex except the O–M–O angle.

#### 4.3. Energetics of the metal complexes

The energetic analysis of all the complexes at B3LYP/6-31G(d)//AM1 level is summarized in Table 3. Binding energies,  $\Delta E$ , are defined as the total energy of complex

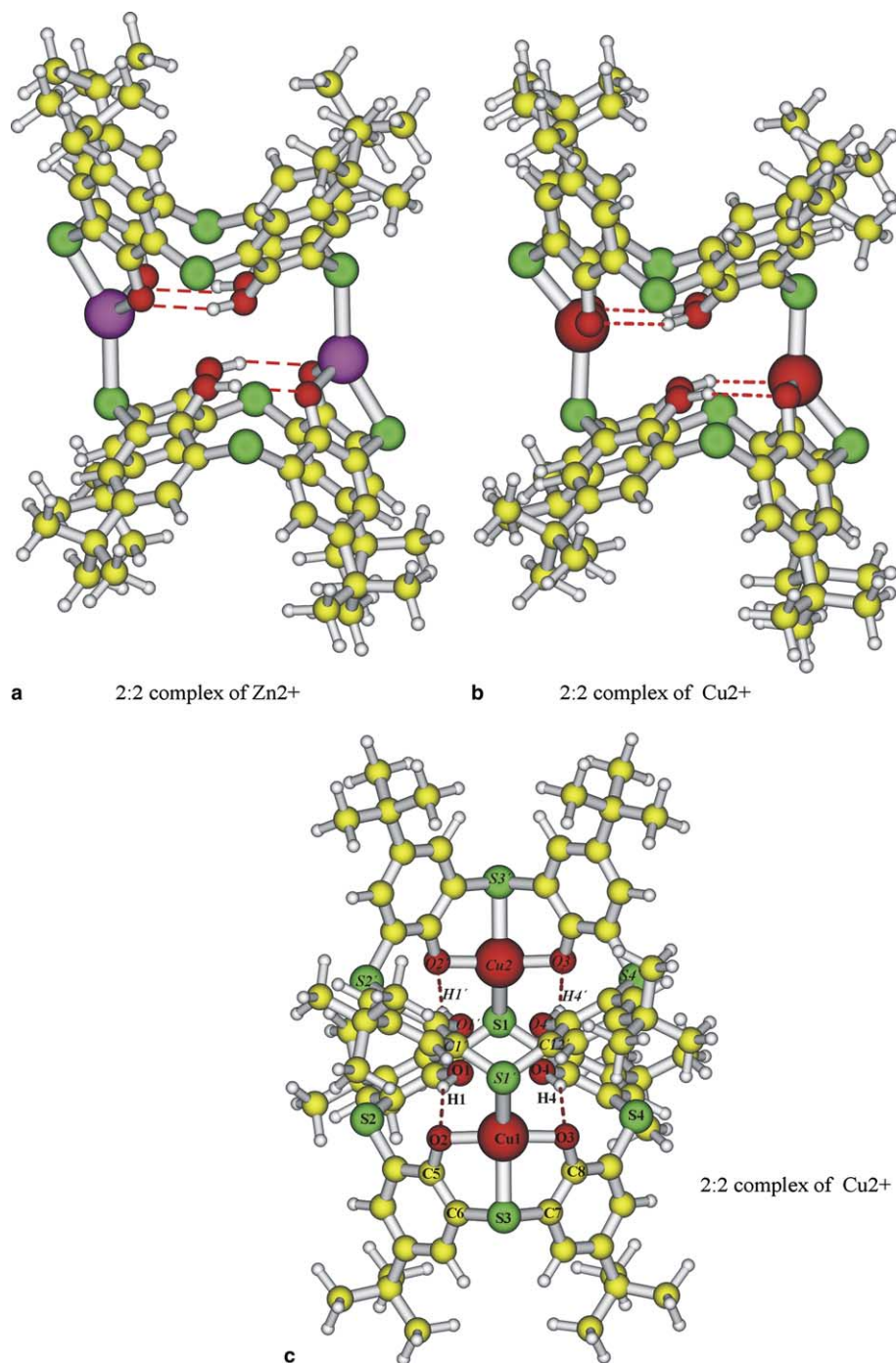


Fig. 6. Optimized structures of each 2:2 metal complex of **3** obtained at AM1 method.

minus the sum of total energies of the most stable isolated moieties, i.e., the metal ion and the opposite phenol twofold deprotonated forms of **1** and **3**. The  $\Delta E$  value of the 1:1  $\text{Cu}^{2+}$  complex with **1** is more negative than  $\text{Zn}^{2+}$ . The coordination of both metals occur preferably in the middle of the lower rim. The  $\text{Zn}^{2+}$  ion prefers to coordinate with two sulfurs and two phenolate groups whereas  $\text{Cu}^{2+}$  ion interacts with two ether oxygens and two phenolate oxygens.

The  $\Delta E$  values of 1st and 2nd possibility of the 1:1  $\text{Zn}^{2+}$  complex of **3** are almost identical whereas in 1:1  $\text{Cu}^{2+}$  complex the  $\Delta E$  value of 1st possibility is lower by about 1.2 kcal/mol. This supports the idea that the migration of the proton in the complex does not influence its stability. Therefore, it is not surprising that a previous theoretical study [15] found only the 2nd possibility in the 1:1  $\text{Zn}^{2+}$  complex of **3**, though, the value of  $\Delta E$  (−647.79 kcal/mol) is different from our study

Table 2  
Structural parameters for the coordination of each complex of **1** and **3** with transition metals at the AM1 level

	Compound <b>1</b>		Compound <b>3</b>								X-ray <sup>a</sup>
	ZnL 1:1	CuL 1:1	ZnLH <sub>2</sub> 1:1 (1st)	ZnLH <sub>2</sub> 1:1 (2nd)	ZnLH <sub>2</sub> 1:1 (3rd)	CuLH <sub>2</sub> 1:1 (1st)	CuLH <sub>2</sub> 1:1 (2nd)	CuLH <sub>2</sub> 1:1 (3rd)	[Zn <sub>2</sub> (LH <sub>2</sub> ) <sub>2</sub> ] 2:2	[Cu <sub>2</sub> (LH <sub>2</sub> ) <sub>2</sub> ] 2:2	ZnLH <sub>2</sub>
<i>Bond distance (Å)</i>											
M–O <sub>1</sub>		2.04						2.04			
M–O <sub>2</sub>	2.07	1.88	2.04	2.04	2.08	1.87	1.87	1.88	2.09 (2.09) <sup>b</sup>	1.89 (1.89) <sup>b</sup>	2.06
M–O <sub>3</sub>		2.04	2.02	2.04		1.86	1.87	2.04	2.09 (2.09)	1.89 (1.89)	2.06
M–O <sub>4</sub>	2.06	1.87			2.08			1.88			
M–S <sub>1</sub>					2.65						
M–S <sub>2</sub>	2.68										
M–S <sub>3</sub>			2.44	2.43	2.65	2.36	2.36		2.50 (2.50)	2.39 (2.39)	2.68
M–S <sub>4</sub>	2.63										
M–S' <sub>1</sub> <sup>c</sup>									2.58 (2.58)	2.46 (2.46)	
<i>Bond angle (°)</i>											
O <sub>1</sub> –M–O <sub>2</sub>		93.0						77.0			
O <sub>2</sub> –M–O <sub>3</sub>		93.0	123.6	120.6		171.3	171.6	101.8	109.0 (109.4)	159.0 (159.0)	96.3
O <sub>3</sub> –M–O <sub>4</sub>		85.5						77.0			
O <sub>4</sub> –M–O <sub>1</sub>		85.5						101.9			
O <sub>1</sub> –M–O <sub>3</sub>		163.1						167.6			
O <sub>2</sub> –M–O <sub>4</sub>	161.9	168.8			161.7			169.3			
O <sub>2</sub> –M–S <sub>1</sub>					97.0						
O <sub>4</sub> –M–S <sub>1</sub>					79.2						
O <sub>2</sub> –M–S <sub>2</sub>	78.8										
O <sub>4</sub> –M–S <sub>2</sub>	95.1										
O <sub>2</sub> –M–S <sub>3</sub>			90.0	90.9	79.3	89.9	89.0		85.5 (85.5)	88.1 (88.1)	76.9
O <sub>3</sub> –M–S <sub>3</sub>			90.0	91.0		87.6	88.5		85.5 (85.4)	88.1 (88.1)	76.0
O <sub>4</sub> –M–S <sub>3</sub>					97.2						
O <sub>2</sub> –M–S <sub>4</sub>	98.6										
O <sub>4</sub> –M–S <sub>4</sub>	80.4										
O <sub>2</sub> –M–S' <sub>1</sub>									110.6 (110.5)	98.3 (98.3)	
O <sub>3</sub> –M–S' <sub>1</sub>									110.5 (110.5)	98.4 (98.4)	
S <sub>1</sub> –M–S <sub>3</sub>					157.4						
S <sub>2</sub> –M–S <sub>4</sub>	157.6										
M–O <sub>2</sub> –C <sub>5</sub>			111.6	110.0		107.8	106.9		115.3 (115.3)	108.3 (108.3)	
M–O <sub>3</sub> –C <sub>8</sub>			107.0	110.1		103.7	106.4		115.3 (115.4)	108.4 (108.4)	
M–S <sub>3</sub> –C <sub>6</sub>			88.7	87.8		86.8	86.5		91.3 (91.3)	88.0 (88.0)	
M–S <sub>3</sub> –C <sub>7</sub>			86.3	87.8		85.2	86.2		91.4 (91.3)	88.1 (88.0)	
M–S' <sub>1</sub> –C' <sub>1</sub>									112.7 (112.7)	110.6 (110.5)	
M–S' <sub>1</sub> –C' <sub>12</sub>									112.7 (112.7)	110.5 (110.5)	

<sup>a</sup> Ref. [16].

<sup>b</sup> The values in parenthesis belong to the other unit of *cone* conformer in 2:2 complex.

<sup>c</sup> The italic characters concern the other unit of *cone* conformer in 2:2 complex.

Table 3

Energetic data for the complexes of **1** and **3** with  $\text{Zn}^{2+}$  and  $\text{Cu}^{2+}$  at B3LYP/6-31G(d)//AM1

Complex	Total energy of metal ion (a.u.)	Total energy of twofold deprotonated species <sup>a</sup> (a.u.)	Total energy of complex (a.u.)	$\Delta E$ (kcal/mol)	$\Delta E_{\text{rel}}$ (kcal/mol)
<b>Compound 1</b>					
1:1 $\text{Zn}^{2+}$ complex	−1778.107014	−4442.046783	−6221.160827	−631.92	–
1:1 $\text{Cu}^{2+}$ complex	−1639.213796	−4442.046783	−6082.340837	−677.87	–
<b>Compound 3</b>					
1:1 $\text{Zn}^{2+}$ complex					
1st possibility	−1778.107014	−3445.615148	−5224.739266	−638.24	0.00
2nd possibility	−1778.107014	−3445.615148	−5224.739238	−638.23 (−647.79) <sup>b</sup>	0.00
3rd possibility	−1778.107014	−3445.615148	−5224.733591	−634.68	3.56
1:1 $\text{Cu}^{2+}$ complex					
1st possibility	−1639.213796	−3445.615148	−5085.904513	−674.93	6.55
2nd possibility	−1639.213796	−3445.615148	−5085.902644	−673.76	7.72
3rd possibility	−1639.213796	−3445.615148	−5085.914952	−681.48	0.00
2:2 $\text{Zn}^{2+}$ complex	−1778.107014	−3445.615148	−10449.563860	−1330.03 (−665.02) <sup>c</sup>	–
2:2 $\text{Cu}^{2+}$ complex	−1639.213796	−3445.615148	−10171.850859	−1376.11 (−688.06) <sup>c</sup>	–

<sup>a</sup> For compound **3**, the opposite deprotonated phenol groups were chosen for the twofold deprotonated species.<sup>b</sup> Ref. [15]. (Binding energies were calculated with respect to optimized structures at B3LYP/6-31G(d) level.)<sup>c</sup> Binding energies per mole of metal ion in parenthesis.

(−638.23 kcal/mol). However, this discrepancy can be explained by two reasons. First, the value obtained from the single point calculation at B3LYP/6-31G(d)//AM1 slightly differs from the previous value obtained with full optimization at B3LYP/6-31G(d) level. Second, our binding energies were calculated with respect to the second deprotonation on opposite phenol groups as the most stable ligand, while the referred value has been calculated with respect to the second deprotonation on adjacent phenol groups.

Binding energies relative to that of the most strongly bound complex in 1:1 complex of **3**,  $\Delta E_{\text{rel}}$ , are also reported in Table 3. The  $\Delta E_{\text{rel}}$  values can propose the stability ordering of 1:1 metal complex for **3**. The stability ordering of the  $\text{Zn}^{2+}$  complexes was predicted to be 3rd possibility < 1st possibility  $\cong$  2nd possibility, whereas the ordering of  $\text{Cu}^{2+}$  complex is modified to 2nd possibility < 1st possibility < 3rd possibility. The most favourable  $\text{Zn}^{2+}$  complex of **3** revealed the coordination pattern via ligation of one bridging sulfur with cooperative binding of the adjacent phenolate groups to form two five-membered chelated rings as corroborated by previous NMR and X-ray structural analysis [9,16]. By contrast, the most stable  $\text{Cu}^{2+}$  complex of **3** adopted a

distorted square planar coordination to the metal ion with the four oxygens (Fig. 5(b)).

All the results support the higher complexation ability of both compounds to  $\text{Cu}^{2+}$  than to  $\text{Zn}^{2+}$ , which agrees well with the previous experiments of metal-ion extractability of **3** [9]. The  $\Delta E$  values of either metal complexes with **3** are more negative than with **1**, which suggest the higher complexation ability of the former compound. Concerning the compound **3**, the  $\Delta E$  values of both the 2:2 metal complexes show higher stability when compared with the 1:1 complexes. This is explained by the increasing binding sites in coordination of the two metal ions.

#### 4.4. Atomic charge distribution

Partial charges of some relevant atoms in both **1** and **3** and in their corresponding  $\text{Zn}^{2+}$  and  $\text{Cu}^{2+}$  complexes were compared and all the information are available as [supplementary material](#). The charge distribution was calculated from the Mulliken population analysis at the same semiempirical method. The results show an increase of negative charge of phenolate oxygens upon the first and second deprotonation of **1** and **3**. Interestingly, the charge of the metal ion is reduced upon complexation which reflects an increase in the charge of sulfur bridging atoms, especially the ones contributing to the binding with metal ions. Consequently, Mulliken analysis indicated some charge transfer from metal to sulfur and oxygen in the complexation, which may suggest an important role in the stabilization of the complexes. The charge distribution of  $\text{Cu}^{2+}$  is more reduced than  $\text{Zn}^{2+}$  in all complexes, which supports the higher complexation ability of the former with both compounds.

Table 4

Percent extraction ( $E\%$ ) for single ion experiments of  $\text{Zn}^{2+}$  and  $\text{Cu}^{2+}$  with ligands **1** and **3**

Metal ion	<b>1</b> $E\%$	<b>3</b> $E\%$	pH
$\text{Cu}^{2+}$	58.4	97.5	7.8
$\text{Zn}^{2+}$	17.5	99.5	7.8

$E\% = D_{\text{M}} \times 100 / (D_{\text{M}} + 1)$ . Experimental conditions: (a) aqueous phase:  $1 \times 10^{-4}$  M  $\text{M}(\text{ClO}_4)_2$ ,  $5 \times 10^{-3}$  M  $\text{NaClO}_4$ , HEPES/NaOH buffer; (b) organic phase:  $1 \times 10^{-3}$  M ligand in  $\text{CH}_2\text{Cl}_2$ .



Table 5

Percent extraction ( $E\%$ ) for competitive experiments from metal ion mixture  $[\text{Co}^{2+}, \text{Ni}^{2+}, \text{Cu}^{2+}, \text{Zn}^{2+} \text{ and } \text{Cd}^{2+}]$  by **1** and **3**

Metal ion	<b>1</b> $E\%$	<b>3</b> $E\%$
$\text{Co}^{2+}$	0	98.1
$\text{Ni}^{2+}$	0	98.4
$\text{Cu}^{2+}$	55.7	97.8
$\text{Zn}^{2+}$	5.6	97.6
$\text{Cd}^{2+}$	0.3	97.5

Experimental conditions. (a) Aqueous phase: mixture of  $\text{Co}(\text{ClO}_4)_2$ ,  $\text{Ni}(\text{NO}_3)_2$ ,  $\text{Cu}(\text{ClO}_4)_2$ ,  $\text{Zn}(\text{ClO}_4)_2$ ,  $\text{Cd}(\text{ClO}_4)_2$ , each  $1 \times 10^{-4} \text{ M}$ ;  $5 \times 10^{-3} \text{ M NaNO}_3$ ; HEPES/NaOH buffer with pH 7.8; (b) organic phase:  $1 \times 10^{-3} \text{ M}$  ligand in  $\text{CH}_2\text{Cl}_2$ .

#### 4.5. Liquid–liquid extraction studies of **1** and **3** towards transition metal ions

Extraction experiments has been performed for the transition metal ions  $\text{Co}^{2+}$ ,  $\text{Ni}^{2+}$ ,  $\text{Cu}^{2+}$ ,  $\text{Zn}^{2+}$  and  $\text{Cd}^{2+}$  using the extraction system metal salt – inert salt– $\text{H}_2\text{O}$ /ligand– $\text{CH}_2\text{Cl}_2$  or  $\text{CHCl}_3$  in order to prove the results of the theoretical calculations on the differences of complex formation of the thiacalix[4]arenes **1** and **3**.

The results of single ion and competitive extraction tests are summarized in the Tables 4 and 5. It is clearly shown that ligand **3** possesses a high extraction efficiency at pH 7.8 towards all metal ions studied. This observation is in a good agreement with the previous literature data [9,10]. In contrast to that the new ligand **1** leads to significant lower extractabilities under identical conditions for these metal ions. But it is interesting to note the lower extraction power of **1** is connected with a remarkable high selectivity for  $\text{Cu}^{2+}$  over  $\text{Zn}^{2+}$  and the other cations. Furthermore, it can be concluded from additional extraction experiments measuring the distribution ratios  $D_M$  of the metal ions ( $D_M = c_{M(\text{org})}/c_{M(\text{w})}$ ) in dependence on both the ligand concentration of **1** ( $\text{LH}_2$ ) and **3** ( $\text{LH}_4$ ) in the organic phase and the pH of the aqueous phase that the extraction reaction is characterized by the 1:1 complex formation (M:L) in the organic phase and the release of two protons into the aqueous phase



with  $n = 2$  and  $4$ .

The corresponding experimental data including the slope analysis for  $\text{Zn}^{2+}$  are given in Supplementary material section.

The extraction results confirm the calculated higher stabilities of the metal complexes with **3** in comparison with **1** and also the preference of the  $\text{Cu}^{2+}$  binding over  $\text{Zn}^{2+}$  by both thiacalix[4]arenes. The differences between theoretical and experimental results in view of the preferred metal complex composition for **3** (2:2 or 1:1 complexes) can be caused by the chosen significant ligand

excess compared with the metal concentration in case of the extraction studies. Such a concentration ratio is necessary in order to keep the activity coefficients of the components constant.

## 5. Conclusion

The structures of neutral and deprotonated species of the cone conformers of **1** and **3** were studied by the semi-empirical AM1 method. To improve the quality of the predicted energies, single point calculations were additionally done at the B3LYP/6-31G(d) level. Two different structures for the twofold deprotonated species were found in **3**, whereas only one was obtained in **1**. The results showed that the structure with two opposite deprotonated phenol groups is more stable than that with two adjacent deprotonated phenol groups. This had never been mentioned in previous studies. The comparative study on the complexation features of **1** towards two different transition metals,  $\text{Zn}^{2+}$  and  $\text{Cu}^{2+}$ , were investigated and also compared with **3** at the same theoretical method. Interestingly, the most stable 1:1  $\text{Zn}^{2+}$  complex with **3** revealed the role of one bridging sulfur atom and two adjacent phenolate groups to form a set of two five membered rings, which agrees well with previous NMR and structural analysis. By contrast, the most favourable 1:1  $\text{Cu}^{2+}$  complex adopted a distorted square planar coordination using two opposite phenolate and two phenol groups. Each 2:2 metal complex of **3** presents a higher stability than the corresponding 1:1 complex, which was evidenced by the more negative binding energies. Concerning compound **1**, each 1:1 metal complex seems to prefer the distorted square planar geometry at the middle of the lower rim using different coordination sites. Two  $\text{O}^-$  and two  $\text{O}$  coordinate the  $\text{Cu}^{2+}$ , whereas  $\text{Zn}^{2+}$  interacts with two  $\text{O}^-$  and two  $\text{S}$ . Interestingly, higher complexation ability of  $\text{Cu}^{2+}$  was found in either complexes of **1** and **3** when compared with the  $\text{Zn}^{2+}$ . This suggests the higher complexation ability of **3** towards both metals. This extensive discussion shows that the AM1 semiempirical method is suitable to study larger metal–ligand complexes in thiacalix[4]arene systems. The experimental results for the extraction ability of **1** and **3** towards  $\text{Cu}^{2+}$  and  $\text{Zn}^{2+}$  also confirmed the higher complex stability of the **3** towards these transition metal ions. This study sheds some light on the understanding of the characteristic host–guest properties of **1** and **3** towards transition metals, especially to revise the general postulated view of coordinated transition metals with **3** (Fig. 1). In particular, **1** is one example of the useful modified thiacalix[4]arene to be used as the core unit in novel lysine dendrimer. This study is expected to explain the complexation properties of lysine dendrimer [28] towards both metals in a forthcoming investigation.



## Acknowledgements

Financial support by the Fundação para a Ciência e a Tecnologia (Lisbon) through Ph.D. scholarship SFRH/BD/7077/2001 is gratefully acknowledged. We also thank Dr. P. Friedel for fruitful discussion on this topic.

## Appendix A. Supplementary data

Supplementary material includes relevant data for both compounds **1** and **3**, namely, geometric parameters of all the neutral and deprotonated species, atomic charges of free ligands and their metal complexes, pH and ligand dependency of extraction ability towards  $\text{Zn}^{2+}$  ion. Material are free of charge and can be found online via ScienceDirect: <http://www.sciencedirect.com>. Supplementary data associated with this article can be found, in the online version at doi:10.1016/j.chemphys.2005.07.024.

## References

- [1] (a) J.M.J. Fréchet, D.A. Tomalia, *Dendrimers and Other Dendritic Polymers*, Wiley, Chichester, 2001;
- (b) S.-E. Stibor, H. Frey, R. Haag, *Angew. Chem.* 114 (2002) 1385;
- (c) A. Zingg, B. Felber, V. Gramlich, L. Fu, J.P. Collman, F. Diederich, *Helv. Chim. Acta* 85 (2002) 333;
- (d) A. Dirksen, U. Hahn, F. Schwanke, M. Nieger, J.N.H. Reek, F. Vögtle, L. De Cola, *Chem. Eur. J.* 10 (2004) 2036.
- [2] (a) J.-M. Lehn, *Supramolecular Chemistry: Concepts and Perspectives*, VCH, Basel, 1995;
- (b) J.W. Steed, J.L. Atwood, *Supramolecular Chemistry*, Wiley, Chichester, 2000.
- [3] R. Cacciapaglia, L. Mandolini, in: L. Mandolini, R. Ungaro (Eds.), *Calixarenes in Action*, Imperial College, London, 2000, p. 241.
- [4] (a) H. Kumagai, M. Hasegawa, S. Miyanari, Y. Sugawa, Y. Sato, T. Hori, S. Ueda, H. Kamiyama, S. Miyano, *Tetrahedron Lett.* 38 (1997) 3971;
- (b) N. Iki, C. Kabuto, T. Fukushima, H. Kumagai, H. Takeya, S. Miyanari, T. Miyashi, S. Miyano, *Tetrahedron* 56 (2000) 1437;
- (c) P. Lhoták, *Eur. J. Org. Chem.* 8 (2004) 1675.
- [5] (a) C. Desroches, C. Lopes, V. Kessler, S. Parola, *Dalton Trans.* 10 (2003) 2085;
- (b) J. Odo, K. Matsumoto, E. Shinmoto, Y. Hatae, A. Shiozaki, *Anal. Sci.* 20 (2004) 707;
- (c) Z.-F. Ye, Z.-G. Pan, W.-J. He, X.-F. Shi, L.-G. Zhu, *J. Incl. Phenom. Macroc. Chem.* 40 (2001) 89;
- (d) P. Lhoták, M. Dudic, I. Stibor, H. Petrickova, J. Sykora, J. Hodacova, *Chem. Commun.* 8 (2001) 731;
- (e) F. Nerumi, N. Iki, T. Suzuki, T. Onodera, S. Miyano, *Enantiomer* 5 (2000) 83;
- (f) Y. Higuchi, M. Narita, T. Niimi, N. Ogawa, F. Hamada, H. Kumagai, N. Iki, S. Miyano, C. Kabuto, *Tetrahedron* 56 (2000) 4659.
- [6] (a) H. Akadas, W. Jaunky, E. Graf, M.W. Hosseini, J.-M. Planeix, A. De Cian, J. Fischer, *Tetrahedron Lett.* 41 (2000) 3601;
- (b) P. Lhoták, M. Himl, I. Stibor, J. Sykora, I. Cisarova, *Tetrahedron Lett.* 42 (2001) 7107;
- (c) D. Appelhans, V. Stastny, H. Komber, D. Voigt, B. Voit, P. Lhoták, I. Stibor, *Tetrahedron Lett.* 45 (2004) 7145.
- [7] R.J. Bernardino, B.J. Costa Cabral, *J. Mol. Struct. (Theochem.)* 549 (2001) 253.
- [8] A. Suwattanamala, A.L. Magalhães, J.A.N.F. Gomes, *Chem. Phys. Lett.* 385 (2004) 368.
- [9] N. Iki, N. Morohashi, F. Narumi, S. Miyano, *Bull. Chem. Soc. Jpn.* 71 (1998) 1597.
- [10] N. Iki, N. Morohashi, Y. Yamane, S. Miyano, *Bull. Chem. Soc. Jpn.* 76 (2003) 1763.
- [11] T. Horiuchi, N. Iki, H. Oka, S. Miyano, *Bull. Chem. Soc. Jpn.* 75 (2002) 2615.
- [12] M.B. Ali, A. Abdelghani, H.B. Ouada, N. Jaffrezic-Renault, R. Lamartine, *Mater. Sci. Eng. C* 21 (2002) 39.
- [13] (a) D.J. Darensbourg, M.W. Holtcamp, *Coord. Chem. Rev.* 153 (1996) 155;
- (b) M.B. Inoue, P. Oram, G.A. de Riquer, M. Inoue, P. Borbat, A. Raitsimring, Q. Fernando, *Inorg. Chem.* 34 (1994) 3528.
- [14] (a) E. Kimura, in: K.D. Karlin (Ed.), *Progress in Inorganic Chemistry*, Wiley, New York, 1994, p. 443;
- (b) R.E. Babine, S.L. Bender, *Chem. Rev.* 97 (1997) 1359;
- (c) D.E. Wilcox, *Chem. Rev.* 96 (1996) 5648.
- [15] V. Ruangpornvisuti, *J. Mol. Struct. (Theochem.)* 683 (2004) 103.
- [16] N. Iki, N. Morohashi, C. Kabuto, S. Miyano, *Chem. Lett.* (1999) 219.
- [17] A. Suwattanamala, A.L. Magalhães, J.A.N.F. Gomes, *Chem. Phys.* 310 (2005) 109.
- [18] B. Wanno, V. Ruangpornvisuti, *J. Mol. Struct. (Theochem.)* 685 (2004) 57.
- [19] M.J.S. Dewar, E.G. Zebisch, E.F. Healy, J.J.P. Stewart, *J. Am. Chem. Soc.* 107 (1985) 3902.
- [20] M.J.S. Dewar, K.M. Merz Jr., *Organometallics* 7 (1988) 522.
- [21] M.J.S. Dewar, Y.C. Yuan, *Inorg. Chem.* 29 (1990) 3881.
- [22] K. Prendergast, T.G. Spiro, *J. Phys. Chem.* 95 (1991) 9728.
- [23] M.E. Zandler, F.D. Zouza, *J. Mol. Struct. (Theochem.)* 401 (1997) 301.
- [24] M. Bräuer, M. Kunert, E. Dinjus, M. Klußmann, M. Döring, H. Görls, E. Anders, *J. Mol. Struct. (Theochem.)* 505 (2000) 289.
- [25] B. Wanno, W. Sang-aroon, T. Tuntulani, B. Polpoka, V. Ruangpornvisuti, *J. Mol. Struct. (Theochem.)* 629 (2003) 137.
- [26] A.A. Voityuk, N. Rösch, *J. Phys. Chem. A* 104 (2000) 4089.
- [27] J.J.P. Stewart, *MOPAC 2002*, Fujitsu Ltd., Tokyo, Japan, 1999.
- [28] D. Appelhans, M. Smet, G. Khimich, H. Komber, D. Kuckling, B. Voit, *New J. Chem.* (submitted).
- [29] J. Baker, *J. Comput. Chem.* 7 (1986) 385.
- [30] A.D. Becke, *J. Chem. Phys.* 98 (1993) 5648.
- [31] C. Lee, W. Yang, R.G. Parr, *Phys. Rev. B* 37 (1988) 785.
- [32] M.J. Frisch, G.W. Trucks, H.B. Schlegel, G.E. Scuseria, M.A. Robb, J.R. Cheeseman, J.A. Montgomery Jr., T. Vreven, K.N. Kudin, J.C. Burant, J.M. Millam, S.S. Iyengar, J. Tomasi, V. Barone, B. Mennucci, M. Cossi, G. Scalmani, N. Rega, G.A. Petersson, H. Nakatsuji, M. Hada, M. Ehara, K. Toyota, R. Fukuda, J. Hasegawa, M. Ishida, T. Nakajima, Y. Honda, O. Kitao, H. Nakai, M. Klene, X. Li, J.E. Knox, H.P. Hratchian, J.B. Cross, C. Adamo, J. Jaramillo, R. Gomperts, R.E. Stratmann, O. Yazyev, A.J. Austin, R. Cammi, C. Pomelli, J.W. Ochterski, P.Y. Ayala, K. Morokuma, G.A. Voth, P. Salvador, J.J. Dannenberg, V.G. Zakrzewski, S. Dapprich, A.D. Daniels, M.C. Strain, O. Farkas, D.K. Malick, A.D. Rabuck, K. Raghavachari, J.B. Foresman, J.V. Ortiz, Q. Cui, A.G. Baboul, S. Clifford, J. Cioslowski, B.B. Stefanov, G. Liu, A. Liashenko, P. Piskorz, I. Komaromi, R.L. Martin, D.J. Fox, T. Keith, M.A. Al-Laham, C.Y. Peng, A. Nanayakkara, M. Challacombe, P.M.W. Gill, B. Johnson, W. Chen, M.W. Wong, C. Gonzalez,

- J.A. Pople, Gaussian 03, Revision A.1, Gaussian, Pittsburgh, PA, 2003.
- [33] H. Akdas, L. Bringel, E. Graf, M.W. Hosseini, G. Mislin, J. Pansanel, A. De Cian, J. Fischer, *Tetrahedron Lett.* 39 (1998) 2311.
- [34] A. Bilyk, A.K. Hall, J.M. Harrowfield, M.W. Hosseini, G. Mislin, B.W. Skelton, C. Taylor, A.H. White, *Eur. J. Inorg. Chem.* (2000) 823.
- [35] G. Mislin, E. Graf, M.W. Hosseini, A. Bilyk, A.K. Hall, J.M. Harrowfield, B.W. Skelton, A.H. White, *Chem. Commun.* (1999) 373.